CMES, vol.6, no.3, pp.245-251, 2004

Nucleation and Propagation of Deformation Twin in Polysynthetically Twinned TiAl

L. G. Zhou[1], **L. M. Hsiung**[2], **and Hanchen Huang**[1]

Abstract: Using molecular dynamics simulations, we study the deformation of polysynthetically twinned (PST) TiAl at room temperature. The simulation cell is pre-strained and thermodynamically relaxed to zero stress, so that no dislocations pre-exist in $\gamma-\alpha_2$ interfaces. A uniaxial compression is then applied along one 1/6<112] direction. Our results show that interfacial dislocation pairs nucleate at the $\gamma-\alpha_2$ interface under the compression. The glide and agglomeration of these dislocations lead to the nucleation of deformation twins from the interface. Based on our studies, twins may nucleate without pre-existing interfacial dislocations. Further we have monitored the propagation of the deformation twin, specifically its interaction with $\gamma-\gamma$ and $\gamma-\alpha_2$ interfaces. The observations show that $\gamma-\alpha_2$ interfaces are stronger obstacles to the twin propagation than $\gamma-\gamma$ interfaces are.

keyword: TiAl, twin, dislocation, interface, molecular dynamics.

1 Introduction

TiAl intermetallic compounds and alloys have been a focus of intensive research, due to their supreme properties at elevated temperatures. In particular, they possess high strength, high stiffness, and excellent environmental resistance at high temperatures [Appel and Wagner (1998)]. In addition, their density is low. Consequently, TiAl compounds and alloys are primary candidates of structural materials in the aerospace industry. A major drawback of the compounds is the lack of ductility and toughness at room temperature. Recent efforts have been focused on the development of dual phase alloys with a refined full lamellar microstructure [Hsiung et al. (2002)]. The two phases are γ-TiAl and α_2-Ti_3Al, plus additional alloying elements. Increased fracture toughness and creep resistance result from the refined lamellar structure [Liu et al. (1996, 1998); Morris and Lip (1997)]. A polysynthetically twinned (PST) TiAl contains only fine lamellae of γ-TiAl and α_2-Ti_3Al [Wegmann et al. (2000); Parthasarathy et al. (2000)]. Such PST TiAl is sometimes referred as a single crystal, although it contains twin boundaries. Because of the lamellar structure, PST crystals are highly anisotropic in mechanical properties. When the loading direction is parallel or perpendicular to the lamellar interfaces, the yield strength is high but the ductility is low. In contrast, along other loading directions the yield strength is low but the ductility is high [Inui et al. (1992)]. This anisotropy is related to the preferred glide of dislocations along interfaces. It is, therefore, possible to design TiAl materials of controllable strength and ductility by orientational alignment of the lamellae. The optimal design is still a target of on-going efforts [Maruyama et al. (1997)].

One of the controlling factors in the optimization is the deformation twin. According to Farenc et al (1993), deformation twins in γ-TiAl result from coordinated glides of a/6<112] partial dislocations. Similar mechanisms have been observed in dual phase TiAl, and the dislocation nucleation at interfaces is correlated with the local stress concentration [Jin and Bieler (1995)]. The twins may coarsen when ledges nucleate and migrate along the twin boundaries [Kim and Maruyama (2003)]. In contrast to grain boundaries, $\gamma-\alpha_2$ interfaces host dislocations due to the mismatch of two phases. These dislocations dissociate into components at the interface. The glissile components, either collectively after pileup at the interface [Hsiung et al. (1997, 2002)] or individually [Zhang and Ye (2003)], propagate away from the interface, leading to twin formation in the matrix. These experimental observations have clearly demonstrated the twin formation, and correlated it with pre-existing dislo-

---

[1] Department of Mechanical, Aerospace & Nuclear Engineering, Rensselaer Polytechnic Institute, Troy, NY 12180, USA

[2] Lawrence Livermore National Laboratory, Chemistry and Materials Science Directorate, P.O. Box 808, L-352, Livermore, CA 94551, USA

cations at the interface. In terms of twinning mechanism in dual phase TiAl, could twins form without pre-existing interfacial dislocations? And, how do the twins propagate? In this paper, we address these two issues using molecular dynamics simulations.

2 Methodology

The molecular dynamics simulations involve four crucial components: setup of the simulation cell, interatomic potential, control of thermodynamic variables, and analysis techniques [Ghoniem and Cho (2002); Liang et al. (2004)]. In the following, we present these four components one by one.

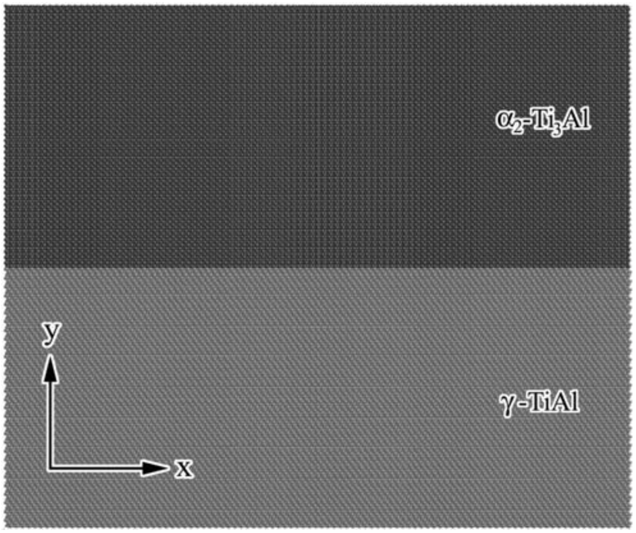

Figure 1 : The simulation cell, with atoms of γ-TiAl shown as light spheres, and atoms of α_2-Ti$_3$Al as dark spheres.

The simulation cell, shown in Figure 1, consists of two slabs, one being the γ-TiAl and the other α_2-Ti$_3$Al. The two slabs form an interface with both side being close-packed planes, that is $(1\bar{1}1)_\gamma//(0001)_{\alpha2}$. Further, the closed-packed directions on the two sides coincide with each other on the interface, that is $<110]_\gamma//<11\bar{2}0>_{\alpha2}$ [Feng et al. (1989)]. The x-axis is along the $[\bar{1}12]_\gamma//[1\bar{1}00]_{\alpha2}$, the y-axis the $[1\bar{1}1]_\gamma$ $//[0001]_{\alpha2}$, and the z-axis the $[110]_\gamma//[11\bar{2}0]_{\alpha2}$. Periodic boundary conditions are applied along all the three directions. The intrinsic mismatches, 2.3% along **x** and 1.5% along **z**, and the corresponding stresses are relaxed through the control of thermodynamic variables; this will be elaborated after the description of interatomic potential. The dimensions of the simulation cell are 50.51 nm along x, 42.45 nm along y, and 2.26 nm along z at 0K; the total number of atoms is 288,000.

Atoms in the simulation cell interact with each other according to a prescribed interatomic potential. The Embedded Atom Method (EAM) potential of Ti-Al [Zope and Mishin (2003)] describes well the stability of multiple Ti-Al phases, and is used in this work. According to this potential, the stacking fault energies of γ-TiAl, which play an important role in the twin nucleation, are 173 mJ/m^2 for the superlattice intrinsic stacking fault (SISF) and 266 mJ/m^2 for the complex stacking fault (CSF); in agreement with experimental and ab initio results [Zope and Mishin (2003)].

With the prescribed interatomic potential, atoms move according to the Newton's equation, under given stresses and temperatures. According to the Parrinello-Rahman algorithm [Parrinello and Rahman (1981)], the size and the shape of a simulation cell respond to the difference of internal and external stresses, so the internal stresses are kept at desired values. We use this algorithm to relax the stress of simulation cell before applying compressive strains. In applying a uniaxial strain, the simulation cell dimension along one direction is varied while other dimensions are fixed. The temperature of the simulation cell is essentially the kinetic energy. We scale the atomic velocities to control the temperature. In contrast to the use of frictional forces, the scaling scheme minimizes impacts of artificial damping forces on defect activities.

Under given stresses (or strains) and temperatures, the molecular dynamics simulations provide details of atomic positions as a function of time. These positions must be analyzed to gain physical insights. The bond-pair analysis technique [Clarke and Jonsson (1993)] provides clear distinction between atoms in perfect crystals, at interfaces, and near dislocations; and it is used in this study. According to this technique, a bond connects two nearest neighboring atoms. The configuration of other bonds formed by the nearest neighbors of the two atoms forming this reference bond determines whether it is good or defected bond. For example, each bond in a perfect face-centered-cubic (FCC) crystal has four ("4") neighboring bonds. Further, atoms in these four bonds form two ("2") other bonds; which are not nearest neighbors to the reference bond. These two bonds form two non-connecting chains, the longest being one ("1") bond in length. This bond configuration is referred to as "421". In the same logic, both 421 and 422 bonds form in hexagonal-close-packed (HCP) crystals. Near an intrinsic stacking fault of FCC structure two layers of atoms are HCP-like, and at a twin boundary only one layer of atoms are HCP-like. In this work, the γ-phase is close to FCC, and the α_2-phase to HCP, and therefore the bond-pair analysis technique applies; and γ and α_2 phases are referred to as FCC and HCP in defect analyses.

3 Results

In this section, we present the mechanisms of twin nucleation and propagation in dual-phase lamellar TiAl compounds, under mechanical loading. Before applying strains, we prepare an interface that is dislocation free.

Some lattice mismatches exist in the initial simulation cell, shown in Figure 1. Using the Parrinello-Rahman algorithm, we relax the internal stress to zero. As shown in Figure 2a, all stress components of the simulation cell go to zeros after 25 ps. After relaxation, the simulation is 50.51 nm along x, 42.73nm along y, and 2.29nm along z. At the end of the relaxation, a twin is formed in the γ-phase, as shown in Figure 2b. The γ-phase is placed in the center by applying the periodic boundary condition in order to better visualize the twin and the $\gamma-\alpha_2$ interfaces. Incidentally, this newly formed twin enables the study of twin interactions, to be presented later.

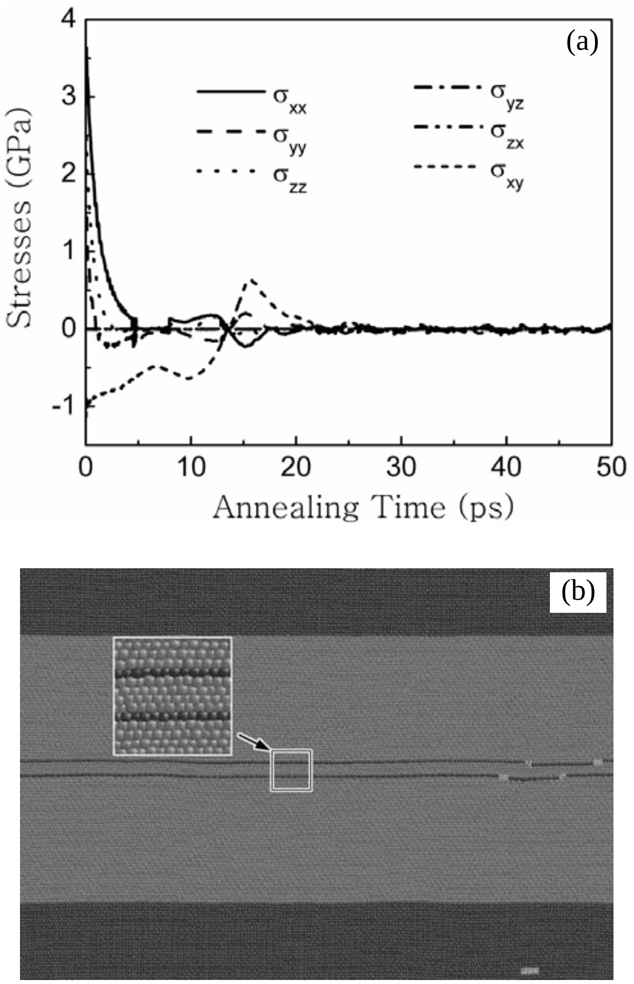

Figure 2 : (a) Stresses during relaxation at 300K, and (b) relaxed atomic configuration (projection on x-y plane), with an expanded view as the inset. The dark, dark gray, and light gray spheres represent HCP atoms, FCC atoms, and other atoms, respectively.

Under a uniaxial strain along the x direction, applied at the rate of $2x10^8$ s^{-1} (that is $2x10^{-7}$ per molecular dynamics step), the atomic configurations in Figure 2b evolve. At 9.3 ps after the loading starts several pairs of interfacial dislocations nucleate at the $\gamma-\alpha_2$ interface, as shown in Figure 3a. In principle, they are nucleated as dislocation loops. However, under the periodic boundary condition, the loops manifest themselves as infinite long dislocations. Even though the interface is dislocation free at the start, the stress application has led to the formation of dislocation pairs. The dislocation formation enables interface migration, which is driven by the strain imbalance. At the end of the stress relaxation, the γ-phase is under tension, and the α_2-phase under compression. The compressive loading compensates the tension in the γ-phase and reduces the strain energy, and its effect in the α_2- phase is the opposite. Consequently, the $\gamma-\alpha_2$ interface migrates into the α_2-phase, to reduce the strain energy, as shown in Figure 3b. Our simulation results reveal two migration mechanisms, depending on which atomic layer near the interface displaces. The atomic packing near a general FCC-HCP interface reads as ABCACAC; with the FCC packing underlined for clarity. The first mechanism is to displace the C layer on the HCP side, leading to the transformation ABCACAC → ABCABCB. This transformation results in two more layers of FCC stacking. The second mechanism is to displace the A layer on the HCP side, leading to the transformation ABCACAC → ABCBABA. This transformation results in an FCC layer sandwiched between two HCP layers. In both cases, the magnitude of layer displacement equals the magnitude of a Shockley's partial. But the Burgers vector directions for the two cases are the opposite.

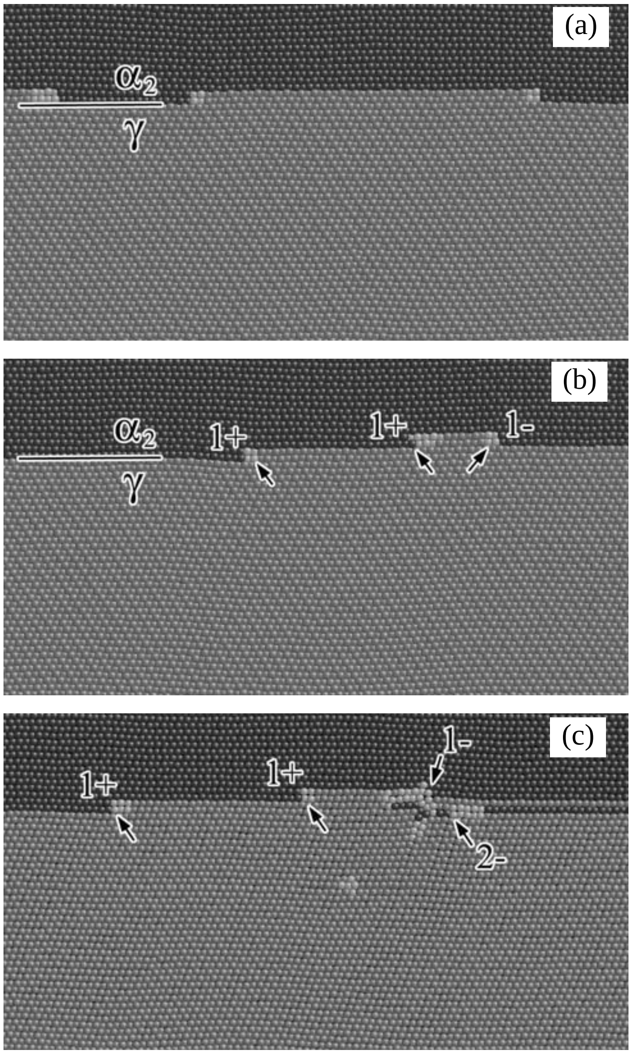

Figure 3 : Nucleation of two types of dislocation pairs at the $\gamma-\alpha_2$ interface, with its initial location indicated by a straight line. The dark, dark gray, and light gray spheres represent HCP atoms, FCC atoms, and other atoms, respectively.

The interface migrations shown in Figures 3a and 3b belong to the first mechanism, and each dislocation pair consists of one "1+" and one "1-" in the figure; the sign "+" and "-" indicate the sense of Burgers vector. The thickness of two atomic layers of the dislocation core is consistent with the experimental observation of Hsiung et al (1997). The second mechanism of interface migration (Figure 3c) involves the second type of dislocation, "2-". As loading continues, the dislocations "1-" and "2-" react, leading to the stress concentration and subsequent emission of a partial dislocation in to the matrix (Figure 4a). The dislocation is emitted to the γ-phase, because of the available slip systems with large Schmid factor. The $(1\bar{1}1)$ cross section view across the dislocation, the inset of Figure 4a, shows that its Burgers vector has no component along the z-axis and is $1/6[1\bar{1}2]$. This method of analyzing dislocation Burgers vector is applied to all cases; although the method will not be explicitly mentioned all the time [Liu et al 2002]. As the second partial dislocation of Burgers vector $1/6[1\bar{1}2]$ is emitted from the same stress concentration, a twin forms (Figure 4b). The remaining dislocation components at the interface react to form a sessile dislocation, which block the glide of other interfacial dislocations. This blockage leads to stress concentration again when other interfacial dislocations arrive, as shown in Figure 4c. The stress concentration triggers the emission of another partial dislocation of $1/6[1\bar{1}2]$ (Figure 4c), and more dislocations (Figure 4d). At this point (Figure 4d), a twin is well developed.

So far our results have shown that a dislocation free $\gamma-\alpha_2$ interface may emit twins. The emission occurs by nucleation of dislocation pairs at the interface, and subsequent emission of partial dislocations from interface to the matrix. Continuation of the uniaxial compressive loading leads to propagation of the twin across a pre-existing twin and a $\gamma-\alpha_2$ interface.

As the load reaches 3.3% compressive strain, the emitted twin propagates toward a pre-existing twin, as shown in Figure 5a. An expanded view of the dislocation front is shown in Figure 5b. The stacking fault generated in the twin shows that a complete dislocation of $1/2[1\bar{1}0]$ has glided through it (Figure 5c); this Burgers vector in the pre-existing twin is equivalent to $1/6[1\bar{1}4]$ in the γ-phase matrix. After going through the twin, the partial dislocation resumes its Burgers vector of $1/6[1\bar{1}2]$. Due to the conservation of Burgers vector in the γ-phase matrix, one dislocation is left at each twin boundary, with Burgers vectors being $1/3[00\bar{1}]$ and $1/3[001]$.

Following the leading partial dislocation is another one that borders the emitted twin. The second partial dislocation follows the footstep of the first in crossing the pre-existing twin. It is interesting to note that the two partial dislocations agglomerate to form twin upon reentering

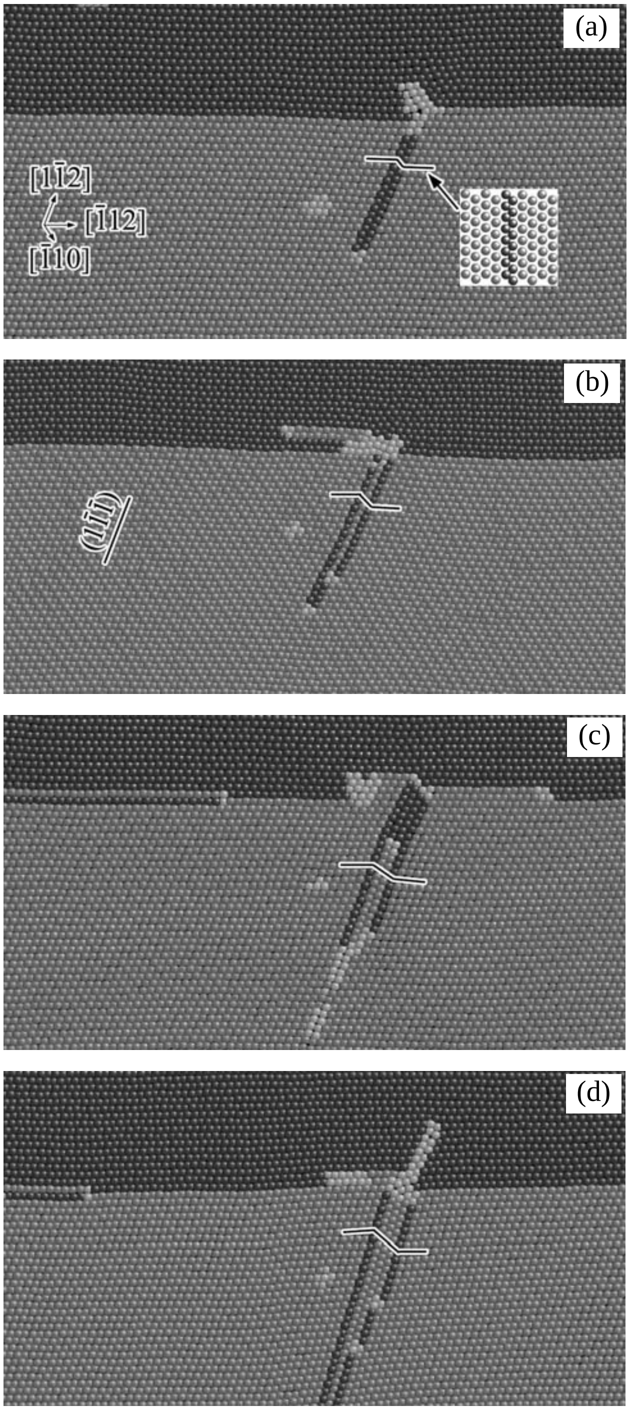
(a)
[1$\bar{1}$2]
[$\bar{1}$12]
[$\bar{1}$10]
(b)
(11$\bar{1}$)
(c)
(d)

Figure 4 : Twin emission from the $\gamma-\alpha_2$ interface, with the atomic alignment near a twin is also indicated by a straight line. The dark, dark gray, and light gray spheres represent HCP atoms, FCC atoms, and other atoms, respectively.

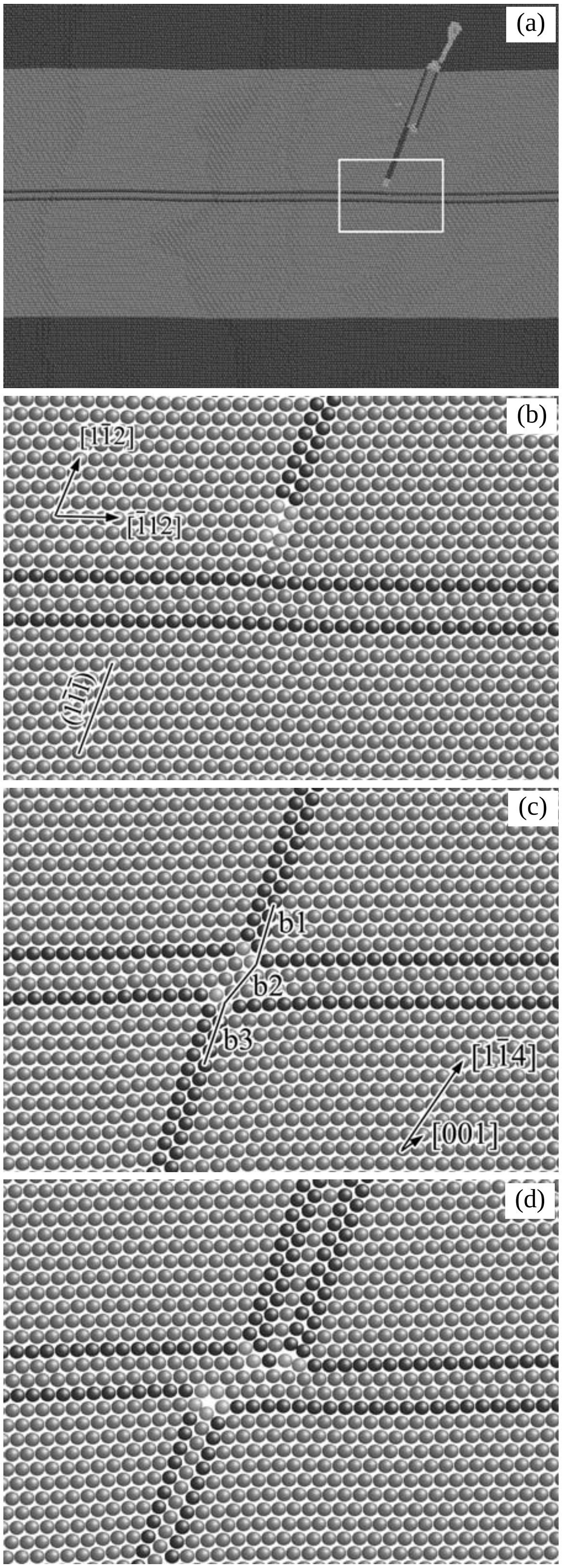
(a)
(b)
[1$\bar{1}$2]
[$\bar{1}$12]
(11$\bar{1}$)
(c)
b1
b2
b3
[1$\bar{1}\bar{4}$]
[001]
(d)

Figure 5 : Twin (and partial dislocations) propagation cross a pre-existing twin.

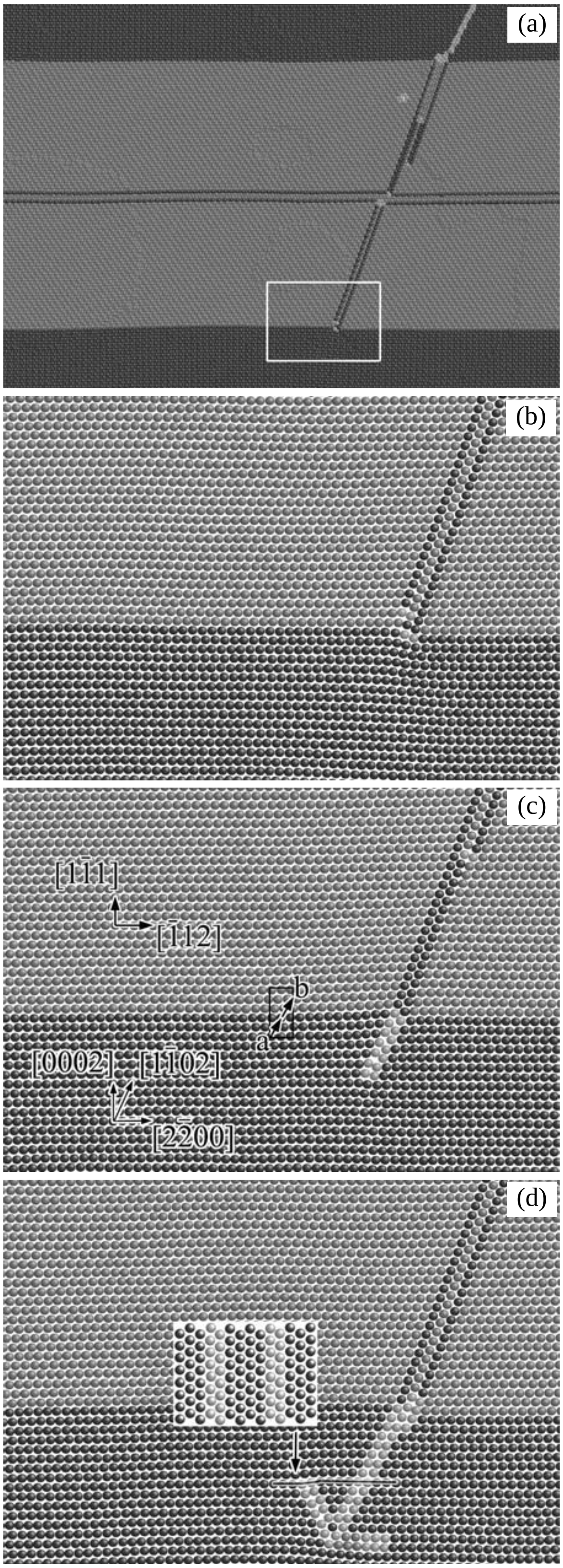

Figure 6 : Interaction of the twin with g - α_2 interface

the matrix (Figure 5d). For comparison, the two partial dislocations are separate before entering the pre-existing twin.

In contrast to the easy penetration of a twin boundary, a $\gamma-\alpha_2$ interface is more difficult for the twin (and partial dislocations) to propagate across. As the strain reaches 3.5% compression, the propagating twin reaches the $\gamma-\alpha_2$ interface, shown in Figure 6a. An expanded view near the interface is shown in Figure 6b. The twin, bordered by two partial dislocations, is unable to propagate across the $\gamma-\alpha_2$ interface. Instead, one of the two partial dislocations is bounced back into the γ-phase, while another one propagates through as a dislocation of Burgers vector $[1\bar{1}02]/4$ (Figure 6c). This Burgers vector (shown as **a** in Figure 6c) is equivalent a vector **b**$=1/24[5\,\bar{5}\,14]$in the γ-phase. Due to the conservation of Burgers vector, a dislocation of Burgers vector $1/24[\bar{1}1\bar{6}]$ is left at the $\gamma-\alpha_2$ interface. Even though one partial dislocation propagates into the α_2-phase, it is unable to propagate through. Instead, this dislocation dissociates into two other dislocations, one going back toward the interface, and another parallel to the interface (Figure 6d). The branching of the dislocation ends the forward propagation of the twin. The results of twin propagation show that it can easily go through another twin in the γ-phase, leaving a $1/3 < 001 >$ dislocation at each twin boundary when a Shockley's partial passes through. In contrast, the twin propagation across a $\gamma-\alpha_2$ interface is more difficult. This difficulty could lead to potential hardening effects.

4 Summary

Our molecular dynamics simulations show that twins may nucleate from a $\gamma-\alpha_2$ interface that is dislocation free and coherent at the start. During uniaxial compression, two types of dislocation pairs form as the interface migrates. When two dislocations from different types of pairs react, stress concentration develops, leading to the emission of partial dislocations and twins into the γ-phase. Further, the debris of the reacting dislocations block further glide of interfacial dislocations along the interface, leading to the emission of more partial dislocations into the γ-phase and thereby the growth of twins. The propagation of twins across a pre-existing twin is easier than across a $\gamma-\alpha_2$ interface.

Acknowledgement: LGZ and HH acknowledge the financial support of Lawrence Livermore National Laboratory. Part of the work was carried out by Lawrence Livermore National Laboratory under the auspices of the US Department of Energy under Contract No. 7405-Eng-48.

References

Appel, F.; Wagner, R. (1998): Microstructure and deformation of two-phase gamma-titanium aluminides. *Mater Sci Eng R*, vol.22, pp. 187-268.

Clarke, A. S., Jonsson, H. (1993): Structural-changes accompanying densification of random hard-sphere packings. *Phys Rev E*, vol. 47, pp. 3975-3984.

Farenc, S.; Coujou, A.; Couret, A. (1993): An insitu study of twin propagation in TiAl. *Philo Mag A*, vol. 67, pp. 127-142

Feng, C. R.; Michel, D. J.; Crowe, C. R. (1989): Twinning in TiAl. *Script Metal*, vol. 23, pp. 1135-1140.

Ghoniem, N. M.; Cho, K. (2002): The emerging role of multiscale modeling in nano- and micro-mechanics of materials. *CMES: Computer Modeling in Engineering & Sciences*, vol. 3, pp. 147-174.

Hsiung, L. M.; Nieh, T. G. (1997): The evolution of deformation substructure in a creep deformed full-lamellar TiAl alloy. *Mater Sci Eng A*, vol. 239-240, pp. 438-444.

Hsiung, L. M.; Nieh, T. G.; Choi, B. W.; Wadsworth, J. (2002): Interfacial dislocations and deformation twinning in fully lamellar TiAl. *Mater Sci Eng A*, vol.329, pp. 637-643.

Inui, H.; Oh, M. H.; Nakamura, A.; Yamaguchi, M. (1992): Room-temperature tensile deformation of polysynthetically twinned (PST) crystals of TiAl. *Acta Metal Mater,* vol. 40, pp. 3095-3104.

Jin, Z.; Bieler, T. R. (1995): An in-situ observation of mechanical twin nucleation and propagation in TiAl. *Philo Mag A*, vol. 71, pp. 925-947.

Kim, H. Y.; Maruyama, K. (2003): Stability of lamellar microstructure of hard orientated PST crystal of TiAl alloy. *Acta Mater*, Vol. 51, pp. 2191-2204.

Liang, H.; Woo, C. H.; Huang, H; Ngan, A. H. W.; Yu, T. X. (2004): Crystalline plasticity on copper (001), (110), and (111) surfaces during nanoindentation. *CMES: Computer Modeling in Engineering & Sciences*, Vol. 6, pp. 105-114

Liu, C. T.; Maziasz, P. J. (1998): Microstructural control and mechanical properties of dual-phase TiAl alloys. *Intermetallics*, vol. 6, pp. 653-661.

Liu, C. T.; Schneibel, J. H.; Maziasz, P. J.; Wright, J. L.; Easton, D. S. (1996): Tensile properties and fracture toughness of TiAl alloys with controlled microstructures. *Intermetallics*, vol. 4, pp. 429-440.

Liu, W. C.; Shi, S. Q.; Woo, C. H.; Huang, H. (2002): Dislocation nucleation and propagation during thin film deposition under tension. *CMES: Computer Modeling in Engineering & Sciences*, vol. 3, pp. 213-218.

Maruyama, K.; Yamamoto, R.; Nakakuki, H.; Fujitsuna, N. (1997): Effects of lamellar spacing, volume fraction and grain size on creep strength of fully lamellar TiAl alloys. *Mater Sci Eng A*, vol. 240, pp. 419-428.

Morris, M. A.; Lipe, T. (1997): Creep deformation of duplex and lamellar TiAl alloys. *Intermetallics*, vol. 5, pp. 329-337.

Parrinello, M.; Rahman, A. (1981): Polymorphic transitions in single-crystals - a new molecular-dynamics method. *J Appl Phys*, vol. 52, pp. 7182-7190.

Parthasarathy, T. A.; Subramanian, P. R.; Mendiratta, M. G.; Dimiduk, D. M. (2000): Phenomenological observations of lamellar orientation effects on the creep behavior of Ti-48at. %Al PST crystals. *Acta Mater*, vol. 48, pp. 541-551.

Wegmann, G.; Suda, T; Maruyama, K. (2000): Deformation characteristics of polysynthetically twinned (PST) crystals during creep at 1150 K. *Intermetallics*, vol. 8, pp. 165-177.

Zhang, J. X.; Ye, H. Q. (2003): The deformation twin in lamellar Ti_3Al/TiAl structure. *Soli Stat Comm*, vol. 126, pp. 217-221.

Zope, R. R.; Mishin, Y. (2003) Interatomic potentials for atomistic simulations of the Ti-Al system. *Phys Rev B*, vol. 68, pp. 024102.